Investigation of the Mechanical Behavior of Locking, Quasi-Locking, and Non-Locking Chains

Eloise Zeng
Co-Worker: Jabri Garcia-Jimenez
Mentors: Chiara Daraio, Wenjie Zhou, Sujeeka Nadarajah

Abstract

Polycatenated Architected Materials (PAMs) represent a new class of materials comprising of topologically interlinked particles, such as rings, polygons, and polyhedra. The mechanical properties of PAMs can be extensively tuned by altering the contact mechanics between individual particles. This study aims to introduce metastability into PAMs through the parametric design of inter-particle contact geometries. These geometries enable a transition between a flexible state, where certain kinematic degrees of freedom are preserved, and a locked state, which restricts any kinematic movement. In this study, we explore two distinct configurations of 1D PAMs, namely the locking chain and the quasi-locking chain, and compared their performance against a conventional non-locking chain. Each chain variant is additively manufactured using thermoplastic polyurethane (TPU), with one set featuring a rough surface and the other a smooth finish. The locking chain exhibits a unique mechanical response; under tensile load, it transitions into a rigid state akin to a solid rod, maintaining rigidity even under lateral shaking. The quasi-locking chain exhibits a similar behavior; however, its links only gently lock into place and can loosen when shaken. In contrast, the non-locking chain behaves like a typical chain, exhibiting no locking behavior. Tensile and compression tests were conducted using the Instron ElectroPuls 3000 apparatus at variable loading rates. These tests facilitated a comprehensive evaluation of force-displacement behaviors and energy dissipation characteristics. The experimental data sheds light on the influence of particle geometry, surface finish, and loading rate on the overall mechanical behavior of the chains. The findings suggest that the locking and quasi-locking chains have potential for applications in robotics and adaptive structural systems, marking a promising avenue for future technological integrations.

Introduction

Metamaterials are materials engineered to have properties rarely seen in naturally occurring materials. A polycatenated architected metamaterial (PAM) is a novel type of material crafted through the interconnection of polygons, polyhedra, or any other closed-loop configurations[1]. Postdoc Wenjie Zhou from Caltech Professor Chiara Daraio's research group in Mechanical Engineering was inspired by the lock-and-key mechanism of enzymes to design a PAM with particles containing lock-and-key mechanisms. This PAM was termed as the “locking chain” because when all the particles are unlocked, they jiggle like particles in a regular chain. When the chain is stretched, its particles squeeze and snap into their locked positions, making the chain rigid like a rubber rod.

I know the design procedure, however, I don’t understand it. Voronoi diagrams are used to describe the behavior of how objects grow e.g. plant cells, giraffe spots, and bubbles. The

objects begin as points; then they grow into circles of increasing radii; once the circles collide with one another, boundaries form. These objects are dubbed as “cells.” The boundary between two cells is equidistant from the center of each cell.

Instead of growing a circle from each point, however, Wenjie grew spheres from two interlinked toruses (Wenjie calls them circles, but his diagram shows toruses).

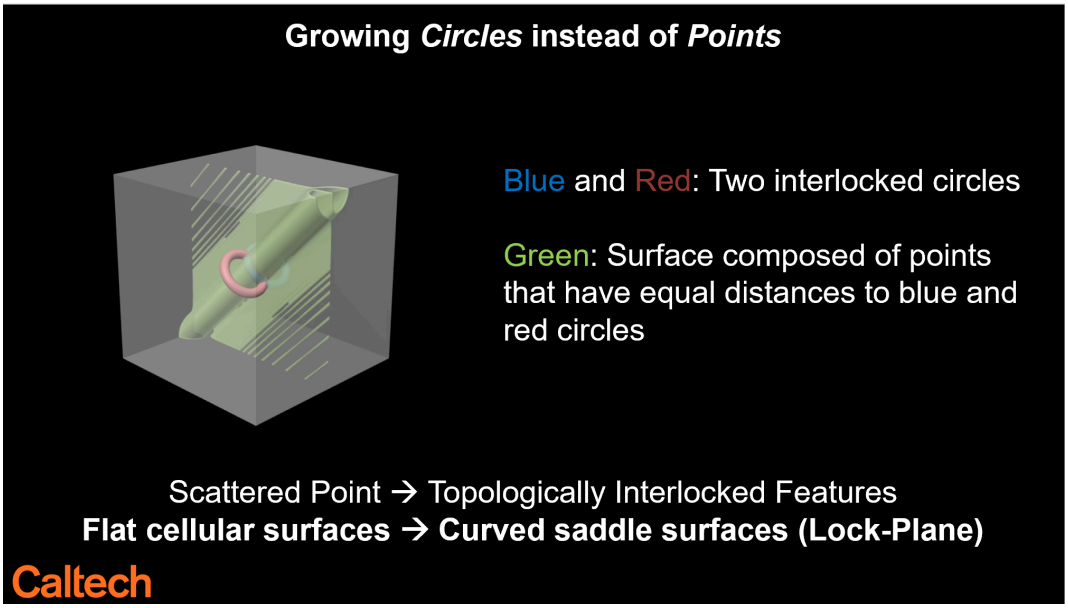

Fig 1. A slide from Wenjie’s presentation.

The cell generated from one torus can be sliced into a “lock-and-key” block.

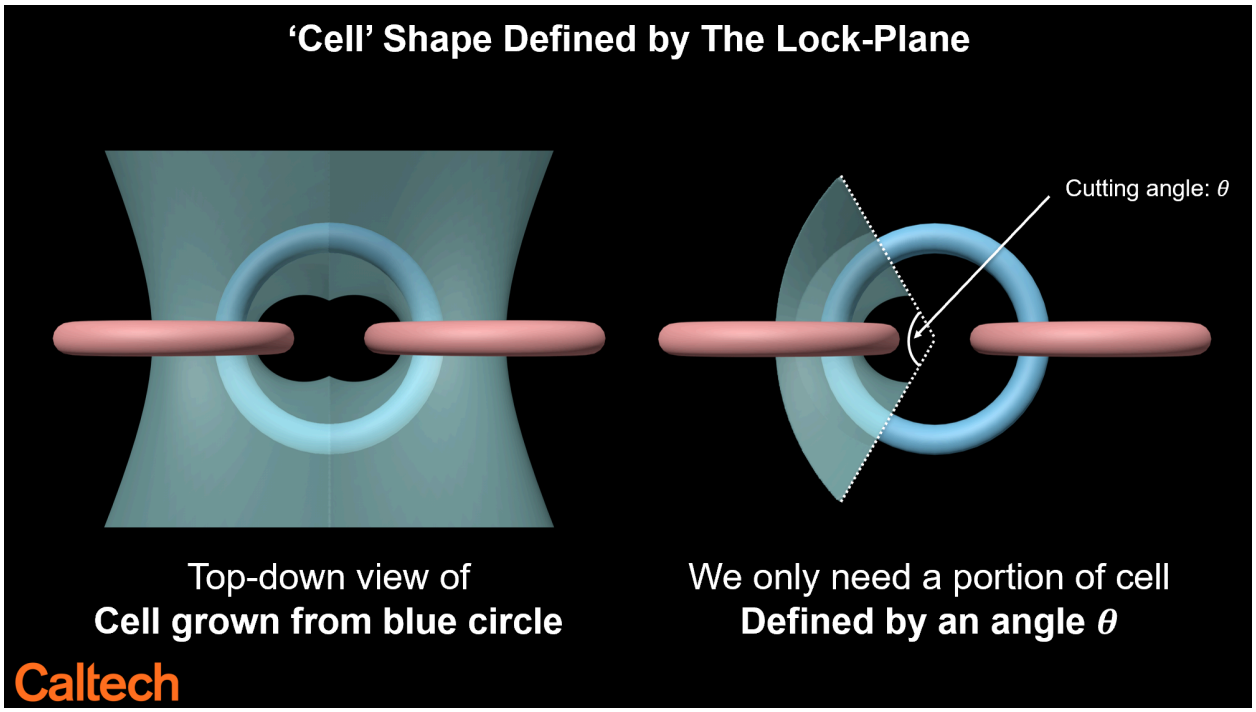

Fig 2. Another slide from Wenjie's presentation.

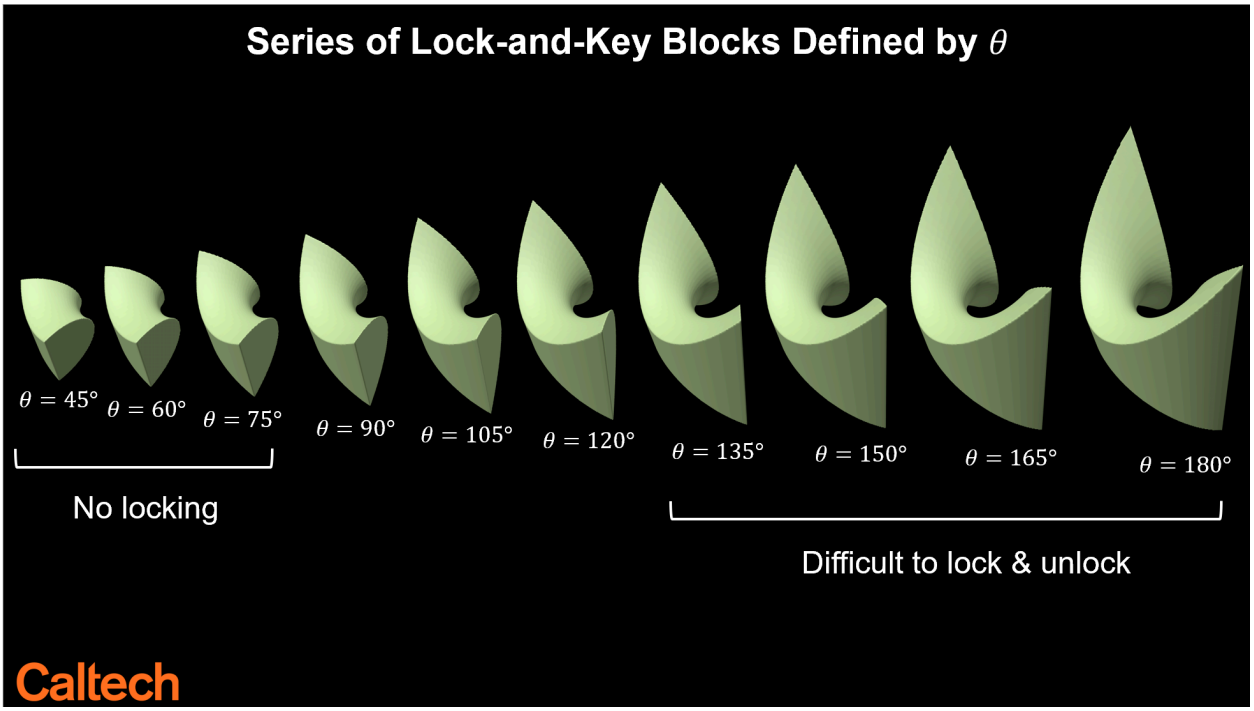

Fig 3. Another slide from Wenjie's presentation.

Each particle in the chain has two lock-and-key blocks formed from various cutting angles. Numerous chains were additively manufactured using thermoplastic polyurethane (TPU). During the process of locking, lock-and-key blocks made from greater cutting angles overlap more than blocks made from smaller cutting angles. Blocks formed by a cutting angle between 135° and 180° were difficult to lock and unlock by hand. Blocks formed by a cutting angle between 45° and 75° exhibited no locking. Thus, we studied three-particle chains with the following cutting angles: 60°, 90°, and 120°. We termed these chains as the non-locking, quasi-locking, and locking chain, respectively. (I don't know how Wenjie knew that growing cells from interlinked circles, then cutting the cells, would create locking mechanisms.)

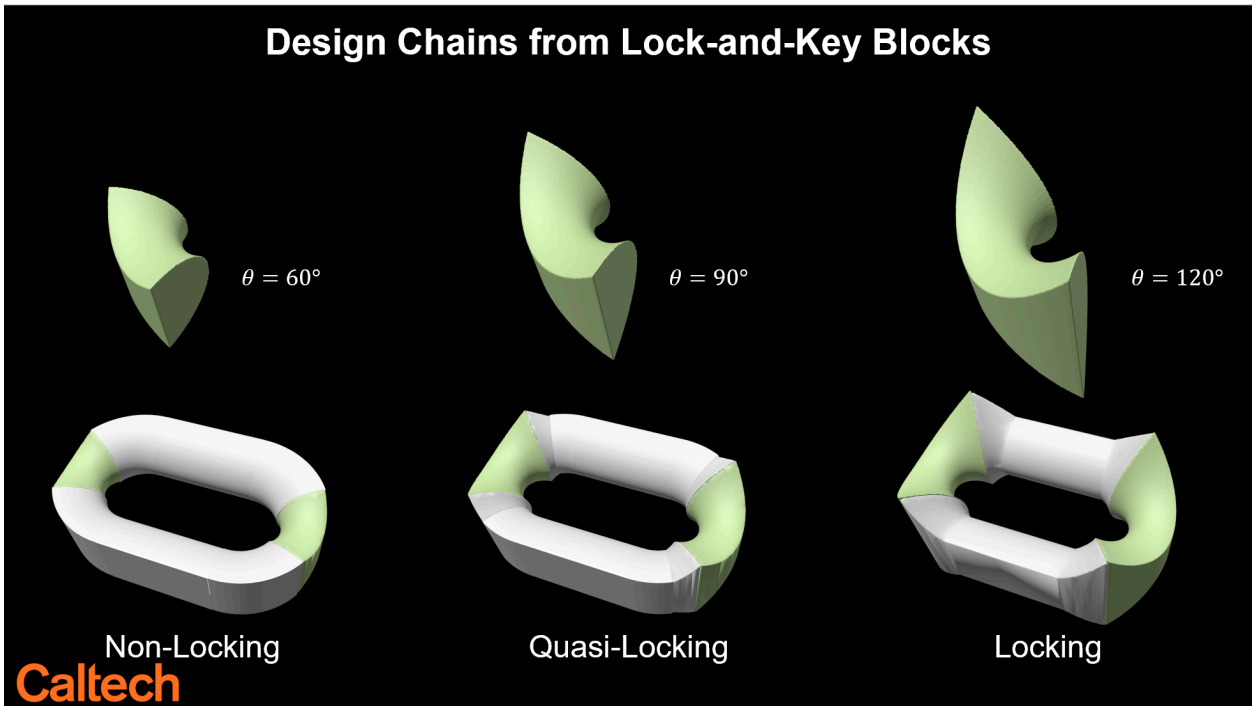

Fig 4. Another slide from Wenjie's presentation.

At the moment, the TPU chains serve no purpose. Locking chains that are tuned to consist of particles of different sizes, materials, and quantities, however, may be useful in future technology. For instance, robots constructed from locking chains may have limbs that can transition from a flexible to rigid state. A robotic snake could move through clustered environments much faster than a humanoid or robotic dog, since the snake can rebound off the obstacles. Furthermore, the snake could climb trees. The robotic snake could transform into something more rigid, like a robotic dog, which could traverse less clustered terrains more quickly.

The locking chain may help cinematographers film more interesting views. For instance, the locking chain could double as a tripod (to film scenes on the ground level) and a rope (for hanging the camera on higher places like a tree branch). Wenjie says the locking chain could also be applied to space tethers (ask him to explain how though).

Studying the locking chains is essential for understanding how to apply them. We tested three-particle chains because three is the minimum number of particles to make a chain. We investigated the tunability of the locking mechanisms by studying the non-locking, quasi-locking, and locking chains. We tested the influence of friction on the chains: one set of these chains has a rough surface finish and the other has a smooth one. The friction coefficients are unknown. We tested the effect of loading rate, the speed at which the chains are stretched, on the chains.

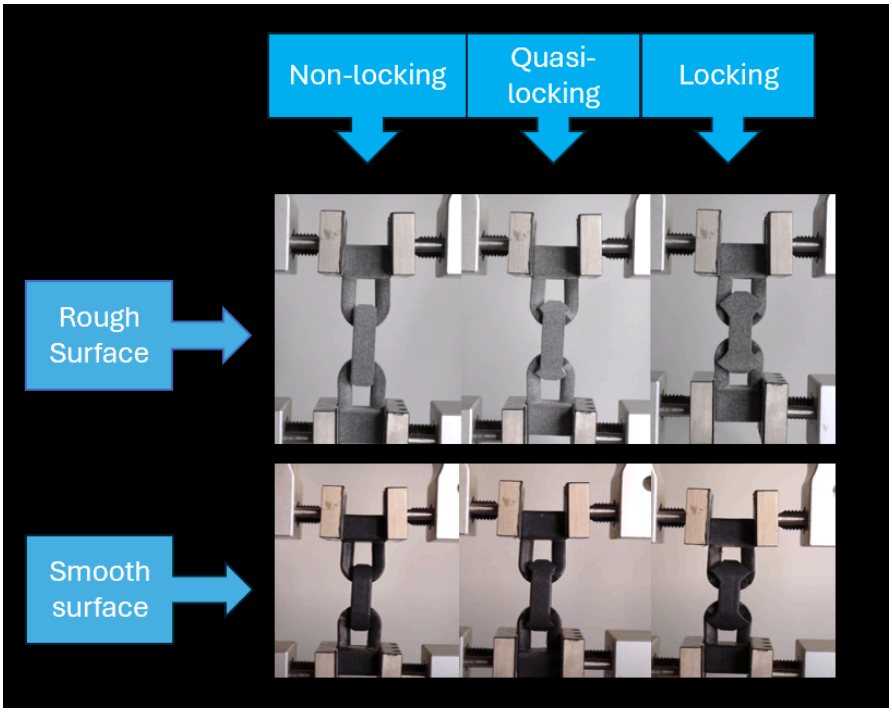

Fig 5. The chains used in the experiment.

Methods

The chain was clamped between two tensile grips. The bottom grip is fixed to the force sensor which is fixed to the Instron Electropuls 3000. The top grip is attached to the top of the machine, and it can move up and down. White strips of tape mark where to place the chains such that they are centered between the grips. A computer recorded the force of the bottom grip vs displacement of the top grip, collecting over one thousand data points per trial (which lasted between 0.5 and 6 minutes). A camera was used to record the experiments. A ring light was used to ensure the speckles on the chain were visible for Digital Image Correlation, a method for analyzing the strain fields of a solid.

An iPhone was used to see if the middle particle was vertical—any misalignment may affect the locking mechanism. The phone holder consists of an 80x20 tube with a bolt through the middle which contacts the metal pole supporting the Instron. The 80x20 tube sits on a paint can, which sits on a cardboard box. We slide an Alan Wrench through the top slot of the 80x20 until the elbow of the wrench is flush with the smallest face of the 80x20. Then we slide the phone against the Alan Wrench and the Instron's pole.

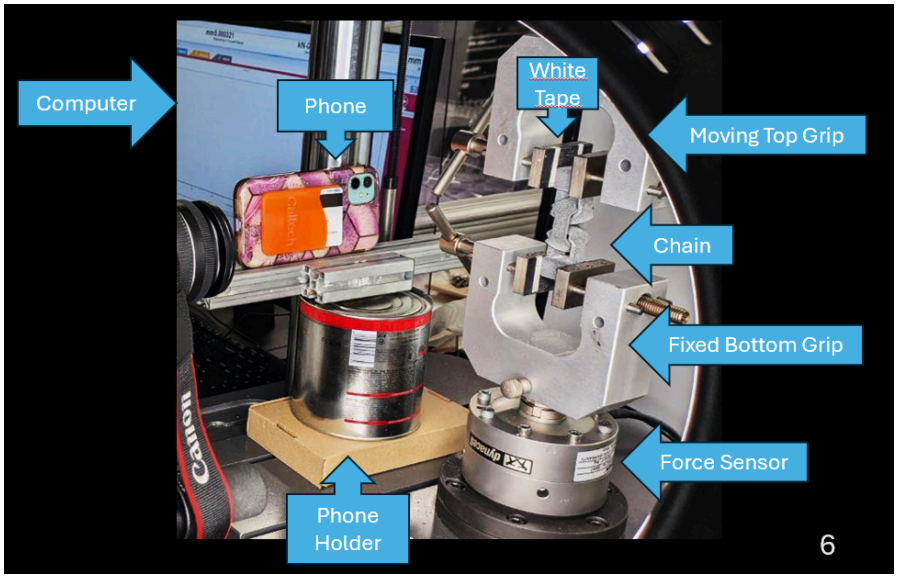

Fig 6. Experimental Setup

We didn't want to stretch a twisted chain, so we built a device for ensuring the front faces of the tensile grips were lying on the same plane. We *duct taped* two black pieces (meant for optics) onto an 80x20 bar. Although the lab has 80x20 all over the place and in many experimental setups, it lacks T-nuts, which can be used for bolting stuff to 80x20 without drilling the 80x20. Instead, people in the lab have primarily been drilling holes through the 80x20, then using regular bolts and nuts. For the drop tower, they inserted the bolt heads into the 80x20 slots, which likely isn't the standard method. Additionally, sliding the bolts creates more friction than using T-nuts. I spotted some T-nuts on some 80x20 hanging above a lab bench though.

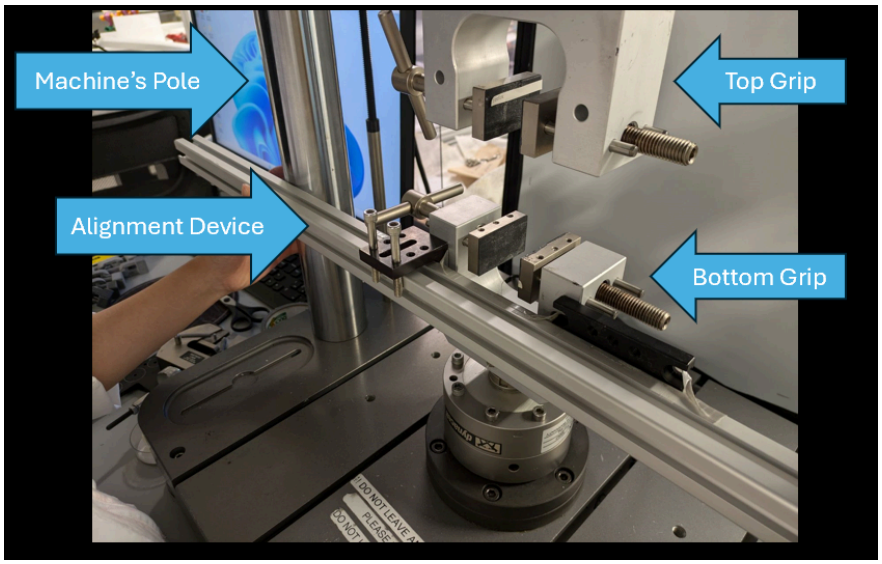

Fig 7. The alignment device.

Experiment 1

The quasi-locking and locking chains were locked and placed on a table. The distance between the top and bottom particles was measured to be 68.1 mm. We call this distance the "Locked Length" of the chain. Similarly, we stretched the non-locking chain till it was taut, then laid it on the table. The distance between its top and bottom particle equaled the locked length of the quasi-locking and locking chains.

For each chain, the Instron stretched the chain from 80% of its locked length to 103% of its locked length—this was called the loading phase. We measured the initial length of the chain using Mitutoyo calipers. Then the Instron compressed the chain to 80% of its locked length—this was called the unloading phase. The loading and unloading rates were 10%, 50%, and 150% of the chain's strain per minute. The force vs displacement graphs were recorded by the machine and plotted in Python. This procedure was repeated until three consistent force-displacement graphs were obtained. The previous trials were termed as the preconditioning trials. Their graphs usually differed from the rest of the trials in a distinct manner.

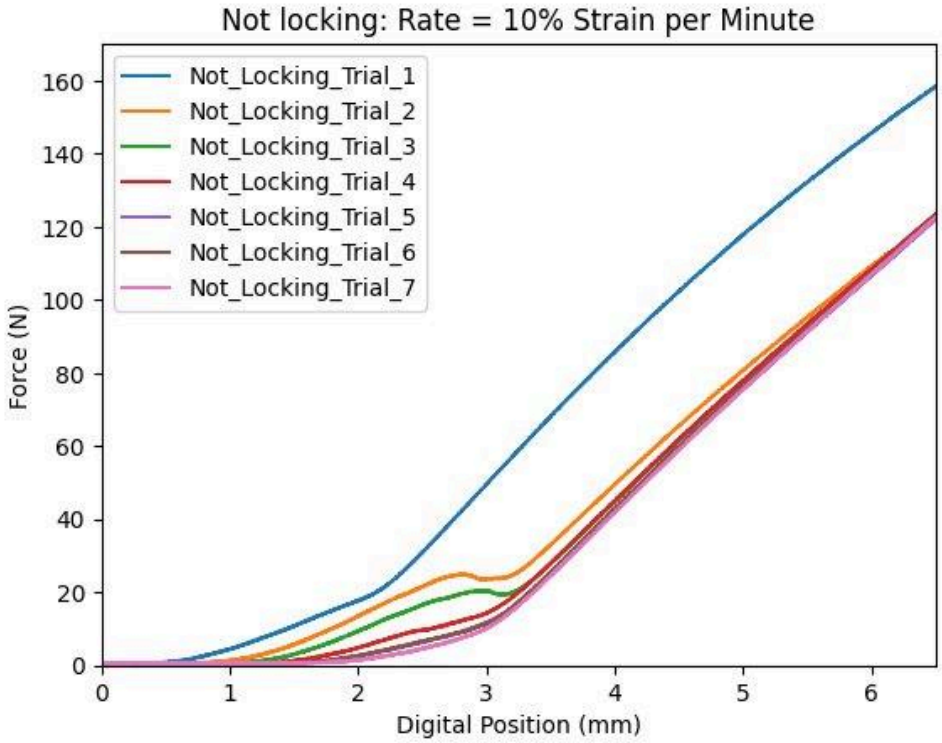

Fig 8. The force-displacement curves for the preconditioning trials vary greatly for the rough non-locking chain.

The loading areas—the area under the curve during the loading phase—were calculated.

Intermediate Results

The rough and smooth locking chains at the various loading rates had force-displacement curves similar in shape and magnitude.

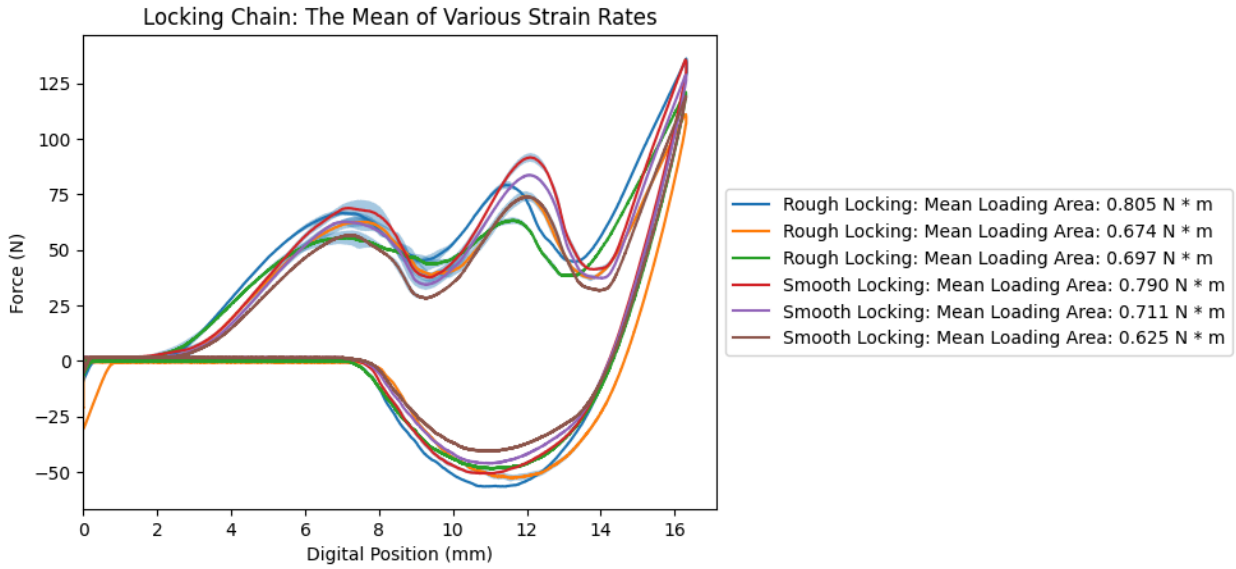

Fig 9. The mean force-displacement curves and their standard deviations for the rough and smooth locking chains.

All the curves had two bumps then a peak during the loading phase.

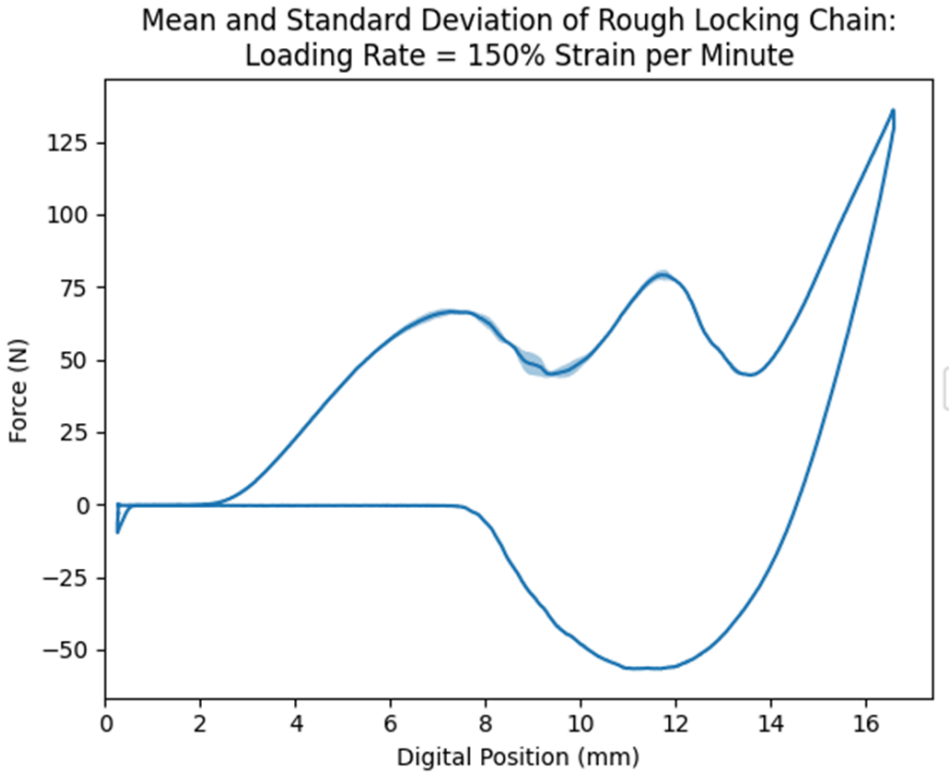

Fig 10. An example of one curve.

I drew a 2D diagram (Fig 11) to explain why we expect two bumps.

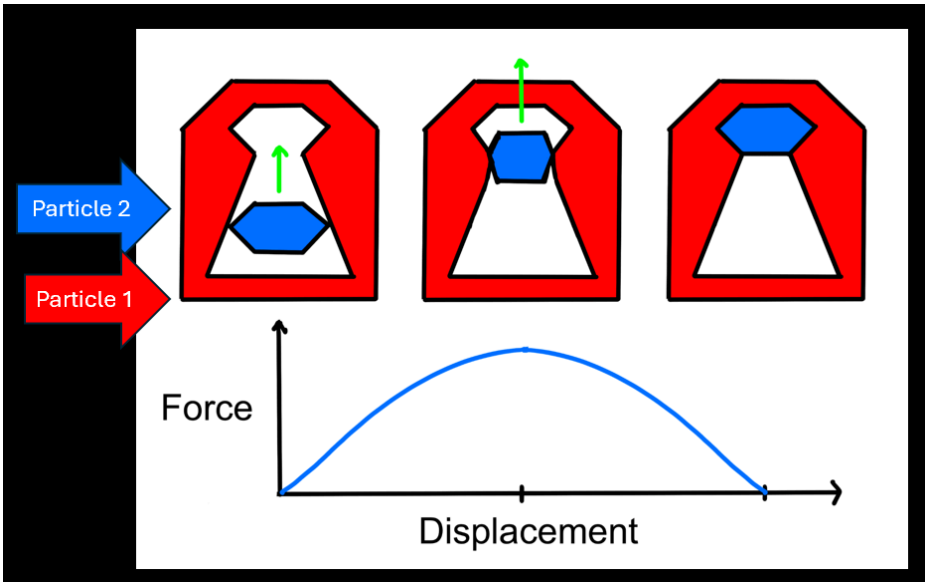

Fig 11. A helpful diagram.

The bottom graph shows the force that particle 1's force sensor measures vs the displacement of particle 2. In the top left diagram, particle 2 is not locked into particle 1. As particle 2 moves upward at a constant velocity relative to particle 1, particle 2 squeezees itself into a more confined region, increasing the friction between particles 1 and 2. Thus, particle 1 feels an increasing upward force. Once particle 2 reaches its most squished position, the force peaks. Once particle 2 passes through, however, the friction between particle 1 and 2 decreases, so the force diminishes. After the particles lock, the force is zero.

Thus, we expected to see two bumps in the force-displacement graph for the three particle chain. The first bump indicates when one particle locks with the middle particle. The second bump indicates when the other particle locks with the middle particle. The second bump has a greater magnitude than the first bump. According to the footage, sometimes the bottom particle locks with the middle particle, then the top particle locks with the middle particle; other times, the order of locking is swapped. This could be due to the initial configuration of the particles. After the chain reaches its locked length, it's stretched even more, causing the final peak in the graph.

In the preconditioning trials for the quasi-locking chains, the force-displacement graphs would have one to two bumps.

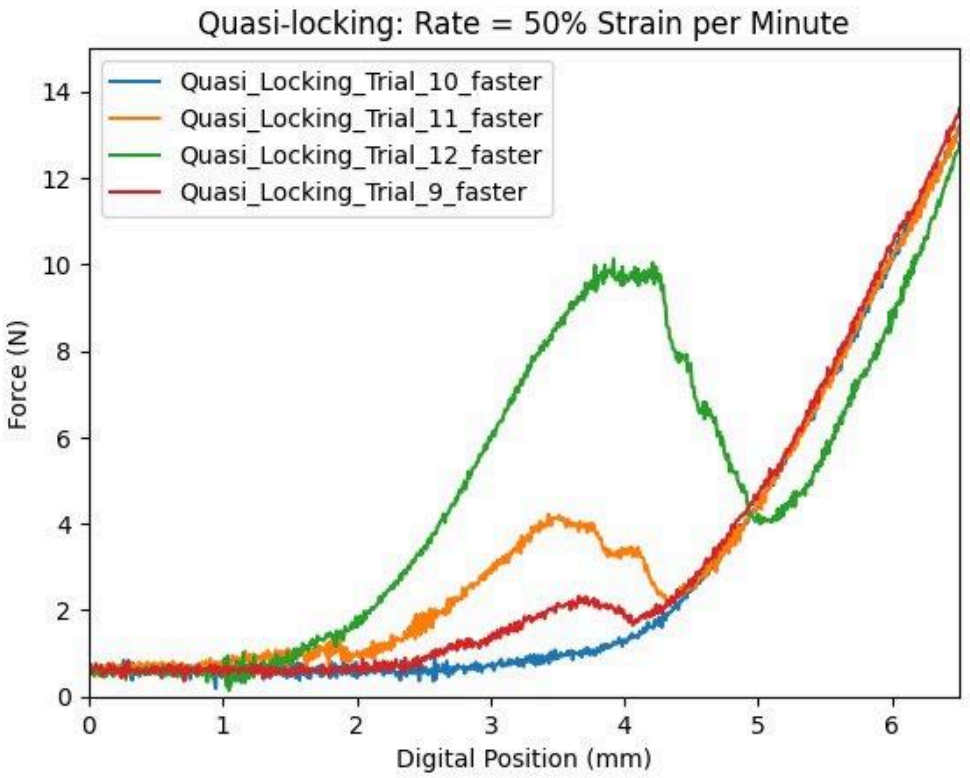

Fig 12. The preconditioning trials for the rough quasi-locking chain.

The degradation of the quasi-locking chains, however, may have caused the lack of bumps in the regular trials.

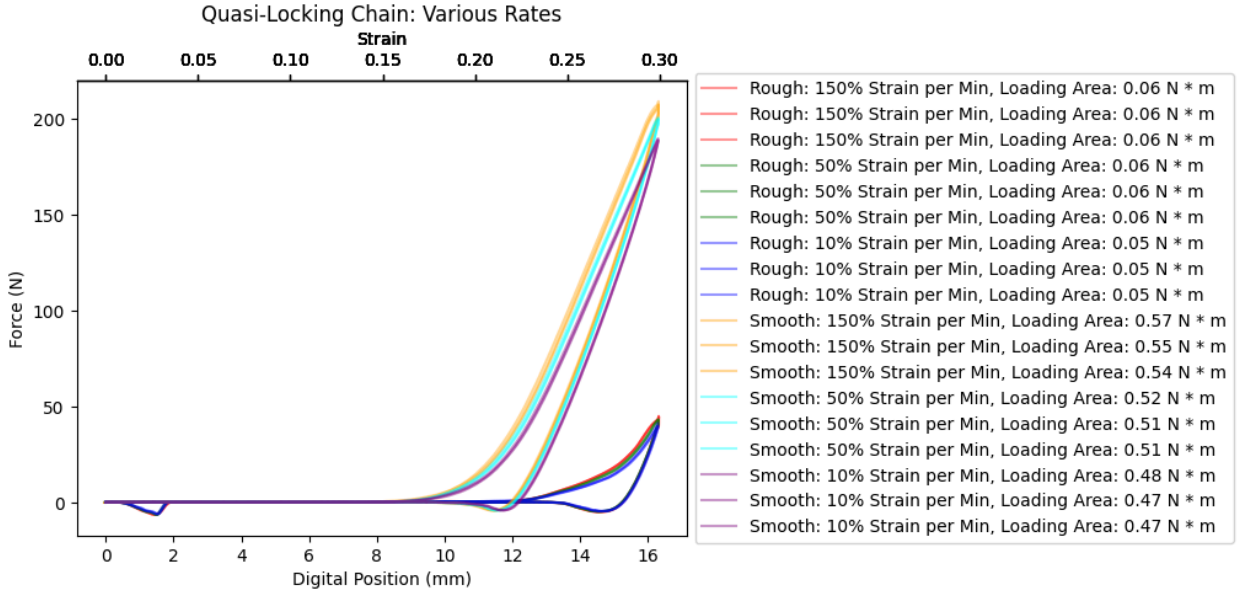

Fig 13. Mean force-displacement curves and their standard deviations for the rough and smooth quasi-locking chain tested at loading rates of 10%, 50%, and 150% strain per minute. The loading phase showcases a smooth curve that transitions into a linear line.

The curves are similar in shape, however, the peak forces between the rough and smooth quasi-locking chains differ by over 100 N.

Similarly, the peak forces between the rough and smooth non-locking chains differed by about 70 N.

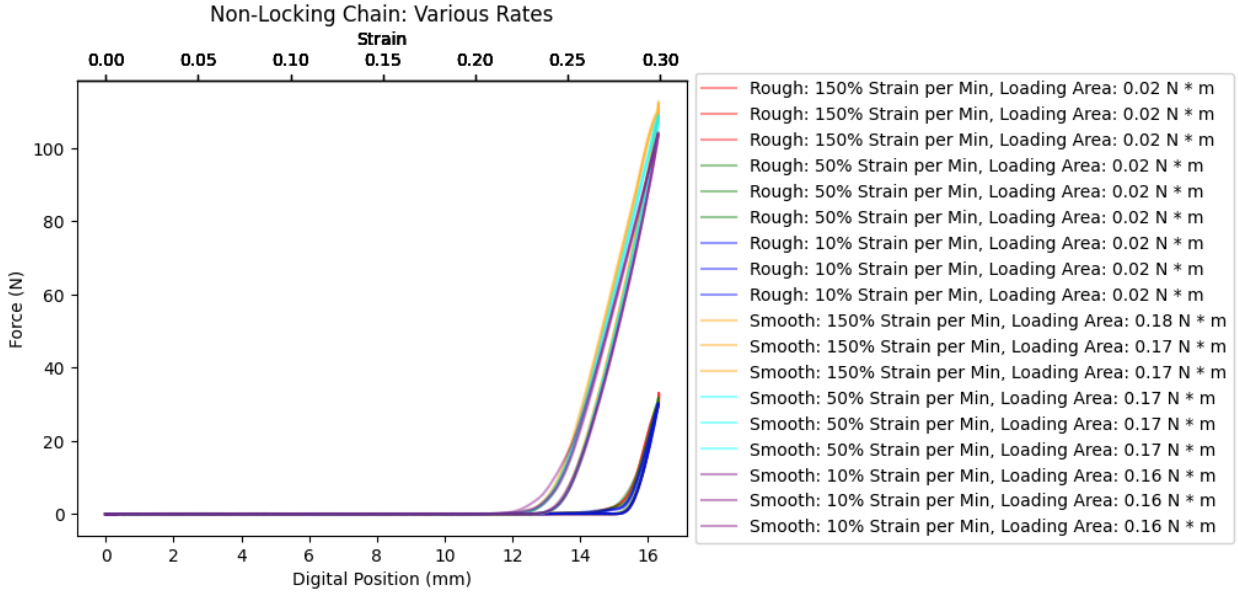

Fig 13. Mean force-displacement curves and their standard deviations for the rough and smooth non-locking chain tested at loading rates of 10%, 50%, and 150% strain per minute. The loading phase showcases a smooth curve that transitions into a linear line.

The differences between the peak forces was surprising because the chains were made of the same material. Thus, we retested the rough quasi-locking chain to see if its peak force could be replicated.

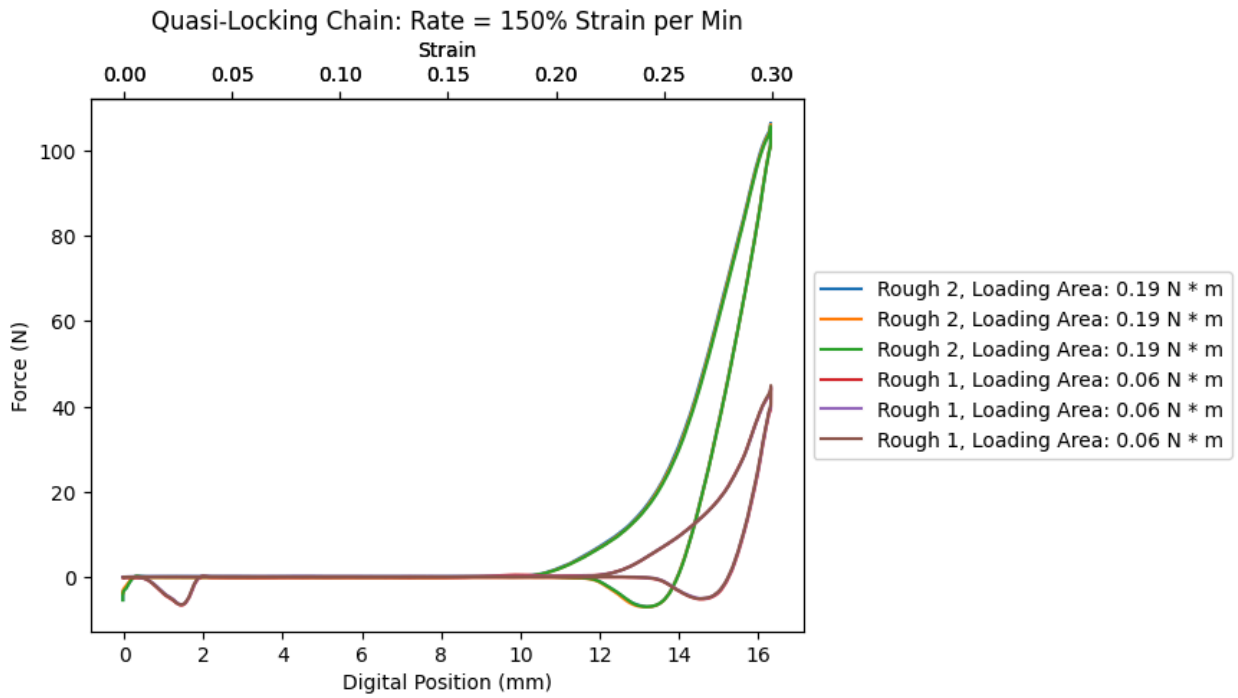

Fig 14. The force-displacement graphs for the rough quasi-locking chain tested on one day vs another day. Three trials were done per day.

It could not. The “Rough 2” trials had a peak force that was about 100 N less than the “Rough 1” trials. Furthermore, the force became positive at a digital position of 12 mm for “Rough 1” and 10 mm for “Rough 2.” This indicated that when measuring the initial length of the chain, there was a 2 mm variation. The force experienced by the bottom particle over a few millimeters of displacement can vary greatly, so we needed another method to accurately compare the force vs displacement graphs between the non-locking, quasi-locking, and locking chains.

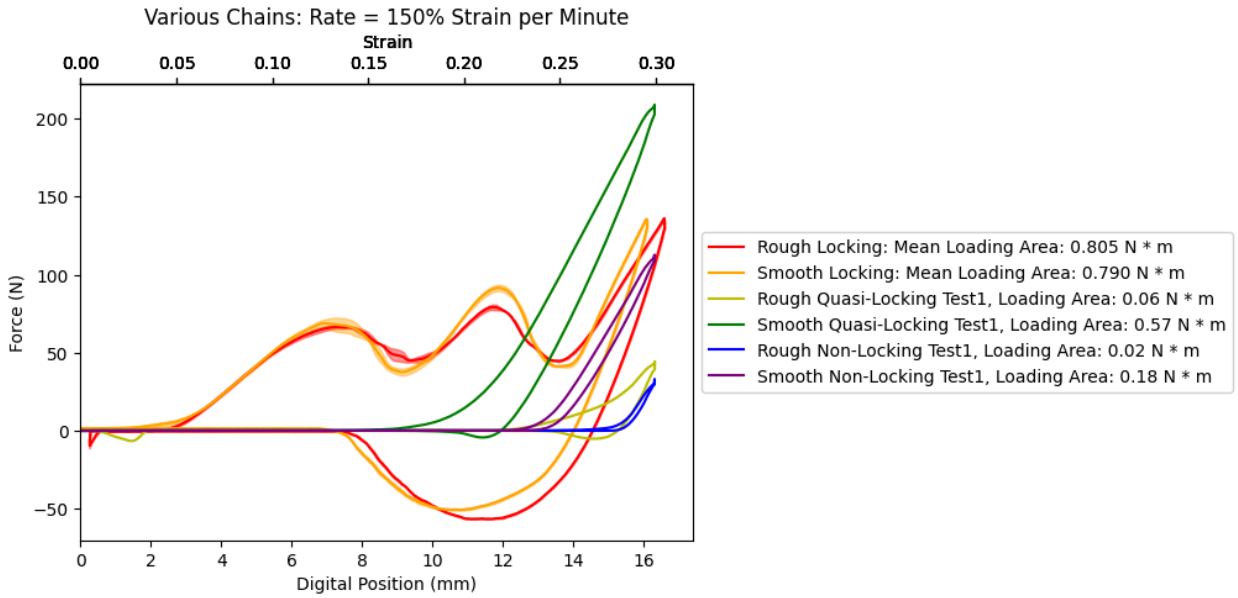

Fig 15. The curves we hoped to align.

Experiment 2

The curves were aligned such that the force becomes non-zero at a displacement of zero. The three types of chains were hung at rest, stretched by 16.3 mm, then compressed to their initial lengths. The loading and unloading rate was 150% strain per minute.

Results

The initial resting lengths of the chains differ. Thus, the non-locking and quasi-locking chains are stretched in their locked position for a far greater displacement than the locking chain. It's much harder to stretch a locked chain than to stretch an unlocked chain. Therefore, the non-locking and quasi-locking chains have far greater peak forces than the locked chain. The peak forces between non-locking and quasi-locking chains are similar regardless of their surface finishes, which suggests our method is replicable.

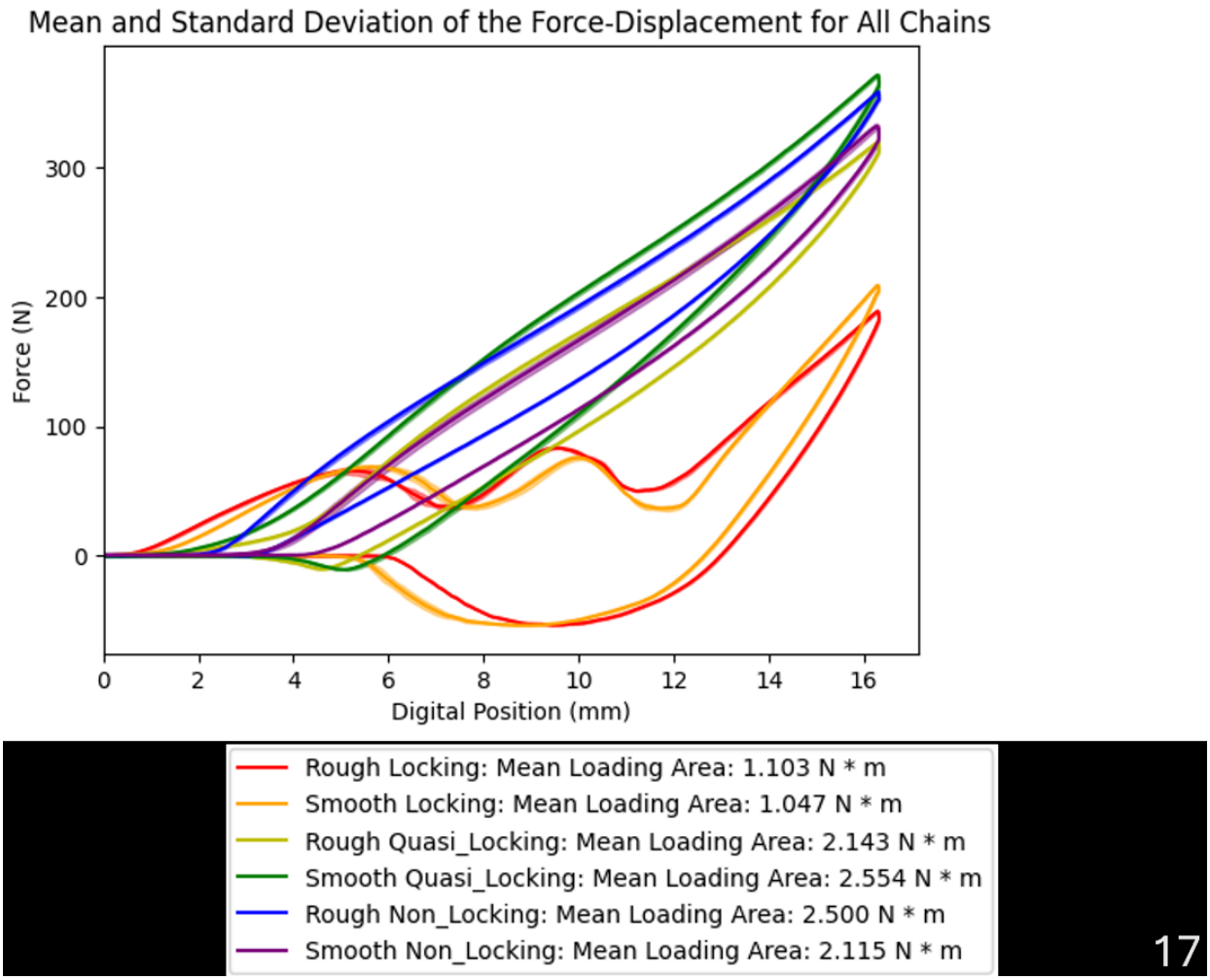

Fig 16. The force-displacement curves generated from experiment 2.

After rewatching the videos, it was realized that the energy dissipated during the locking phase could be calculated. The locking phase begins once all adjacent particles are contacting each other. The phase ends once the chain has reached its locked length.

It's presumed the chain starts unlocking when the force becomes negative. Further studies are needed to confirm this. It's possible that the locking chain locks at the displacement at which the second local minima in the force is reached. This displacement, however, doesn't align with the displacement at which the force becomes negative. The displacements are close though. Furthermore, the length of the quasi-locking chain hanging at rest was measured to be 65.2 mm. Its locked length is 68.1 mm. Hence, the chain should lock at a displacement of around 3 mm. The force, indeed, becomes negative at around 3 mm.

At the displacement that unlocking begins, the chain is at its locked length. The energy dissipated during the locking phase is the area under the curve from the displacement of zero to the displacement at the locked length.

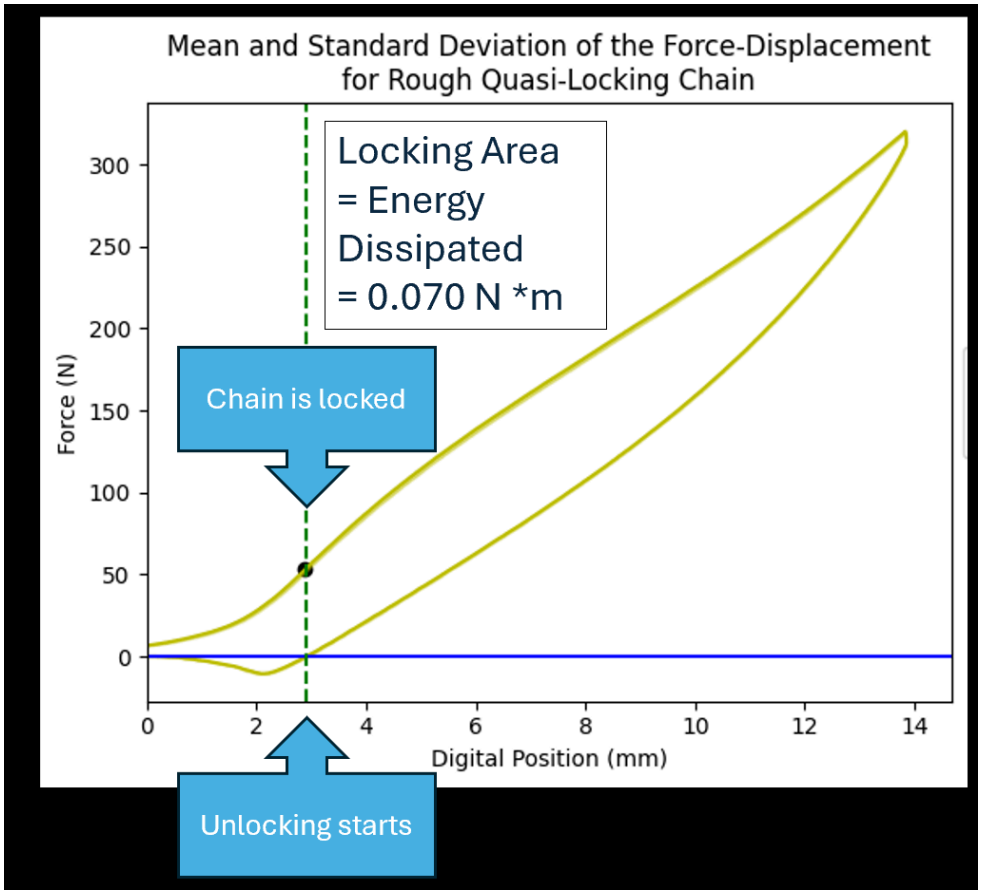

Fig 17. The quasi-locking chain starts unlocking at around 3 mm.

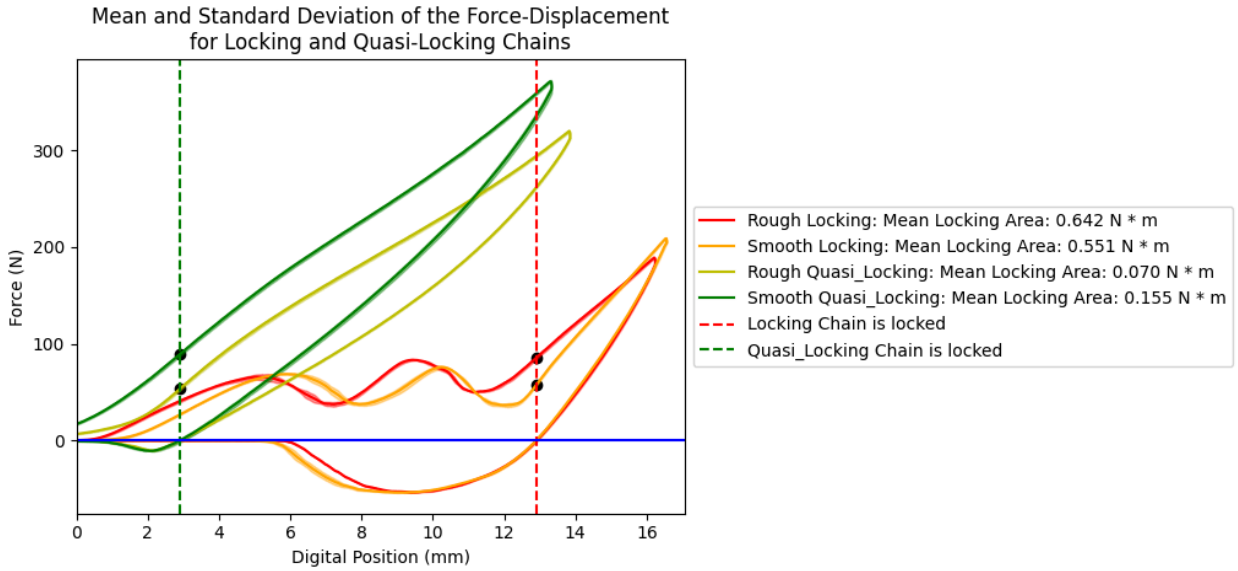

Fig 18. Black points indicate the force and displacement at which the locking and quasi-locking chains are locked.

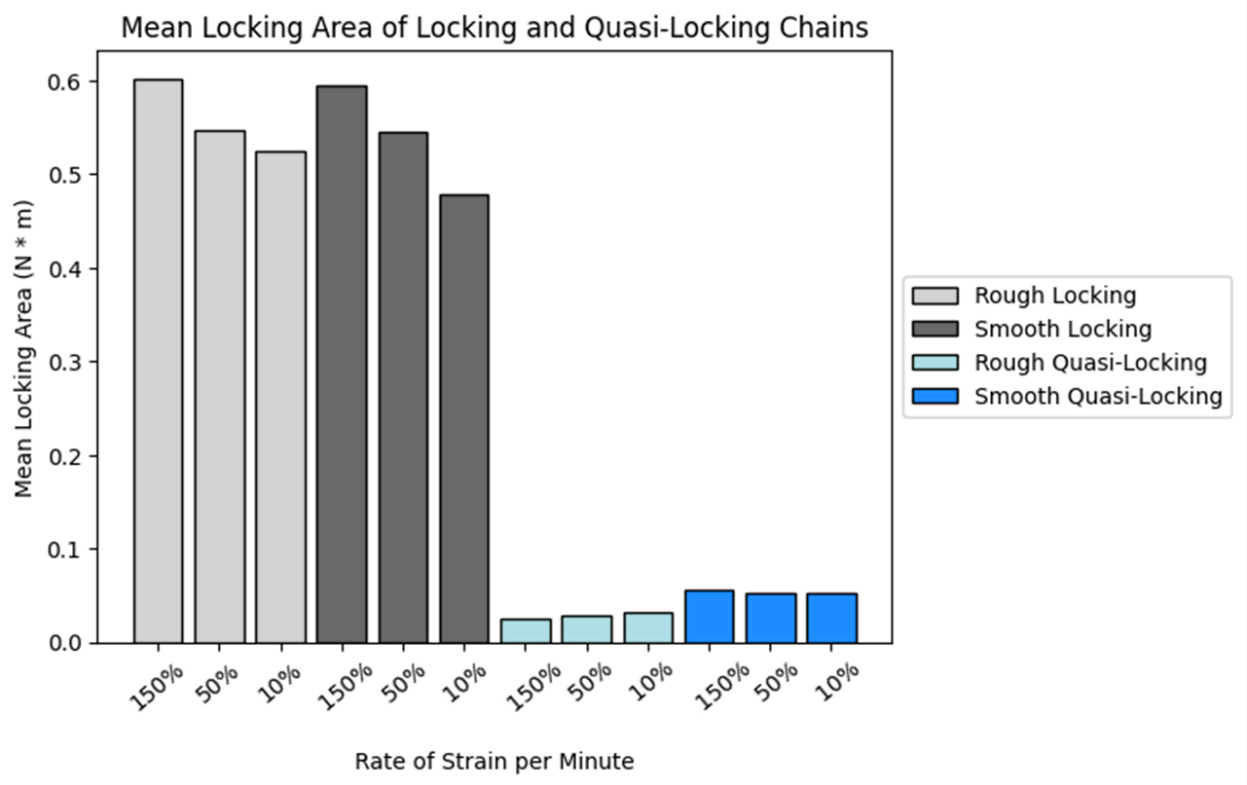

Fig 19. The mean locking area, aka the mean energy dissipated during the locking phase, for the Rough and Smooth Locking and Quasi-Locking Chains tested at various loading rates.

For the locking chains and smooth quasi-locking chain, as the loading rate increased, the energy dissipation increased, although not significantly. For chains with the same friction and geometry, the percentage difference in energy dissipation between trials with a loading rate of 150% and 10% strain per minute was calculated. The maximum percentage difference was 23%.

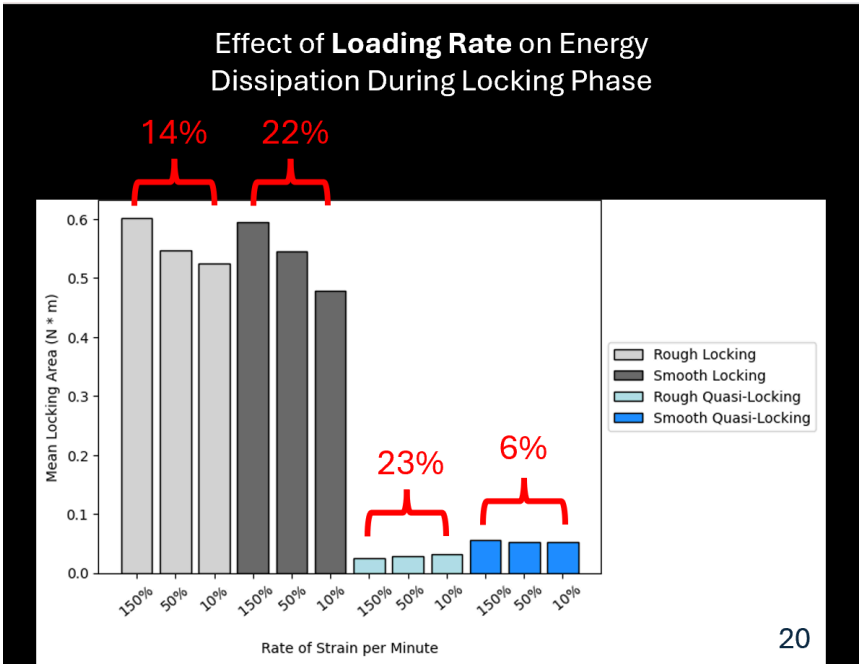

Fig 20. For chains with the same friction and geometry, the percentage difference in energy dissipation between trials with a loading rate of 150% and 10% strain per minute was calculated.

The rough locking chain dissipates more energy than the smooth locking chain, which makes sense because it takes more force to stretch a chain with more friction. The rough quasi-locking chain, however, dissipates less energy than the smooth quasi-locking chain, which indicates experimental error occurred. The percentage differences in energy dissipation between locking chains tested with the same loading rates was calculated. The largest percentage difference was 9%, occuring at a rate of 10% strain per minute.

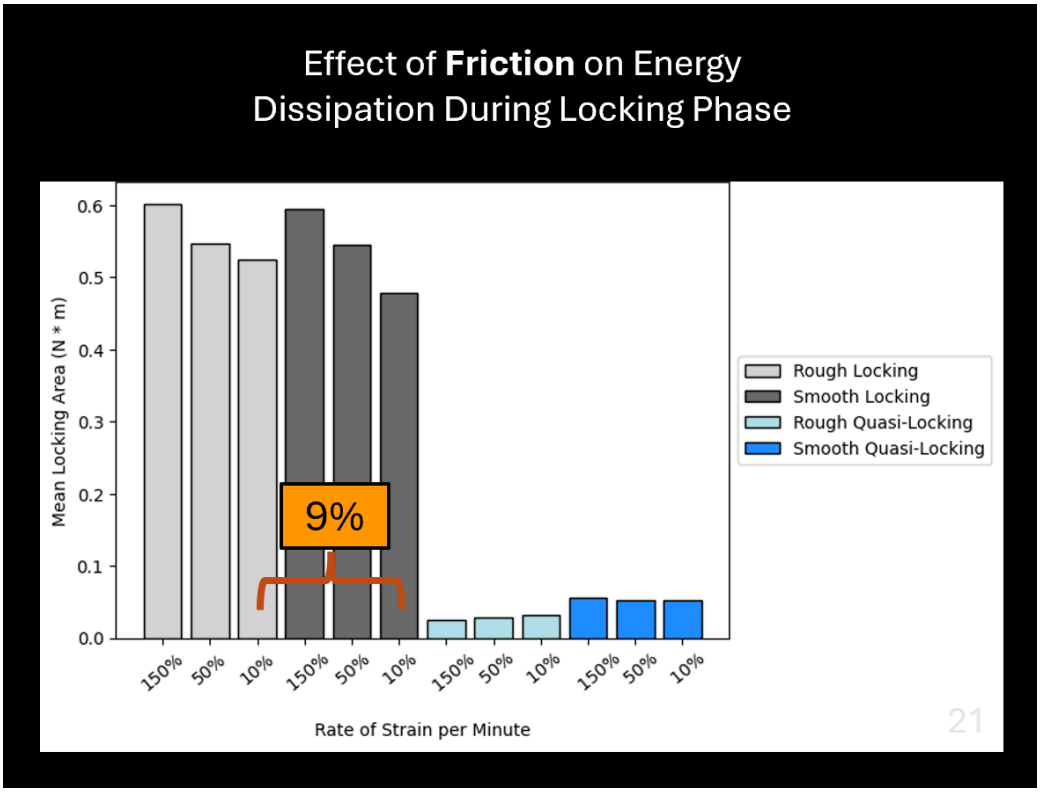

Fig 21. The percentage differences in energy dissipation between locking chains tested with the same loading rates was calculated. Solely the maximum percentage difference is shown. Percentage differences were not calculated for quasi-locking chains since experimental error is probable.

The percentage differences in energy dissipation between chains with the same loading rates and frictions but different geometries was calculated. The smallest percentage difference was 160%, which occurred between smooth locking and quasi-locking chains stretched at a loading rate of 10%. The smooth locking chain dissipated nine times more energy than the smooth quasi-locking chain.

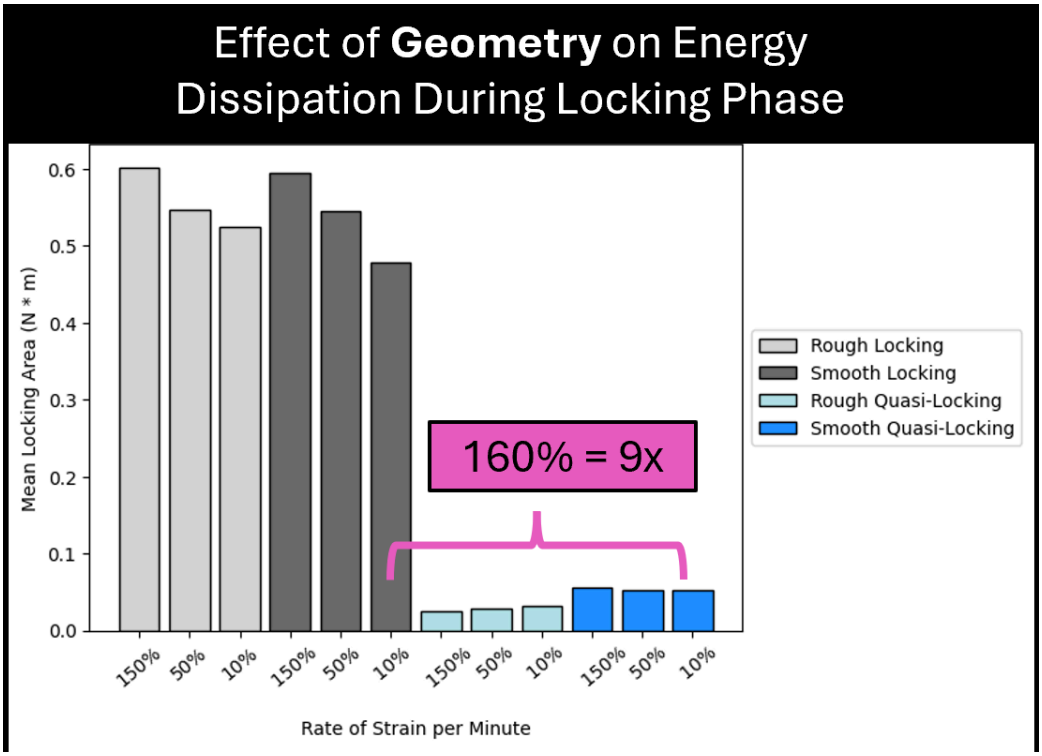

Fig 21. The percentage differences in energy dissipation between chains with the same loading rates and frictions but different geometries was calculated. Solely the minimum percentage difference is shown.

Discussion

The positive correlation between loading rate and energy dissipation agrees with literature regarding other materials such as coal[2] and 2D simulations of granular solids[3]. Further studies are needed to understand the correlation regarding TPU.

The loading rates and friction affect the energy dissipation far less than the geometry of the chains. This suggests the geometry of the chains can be tuned such that chains have specific energy barriers before locking. This analysis, however, is accurate only for the loading rates and surface finishes that were tested. More extreme loading rates and frictions may have a far greater impact on energy dissipated than the geometry of the chain. Further studies should be done to discern how to use the locking chains in future applications.

References

1. Wenjie Zhou, Sujeeka Nadarajah, Liuchi Li, Anna G. Izard, Aashutosh K. Prachet, Payal Patel, Hujie Yan, Xiaoxing Xia, & Chiara Daraio. (2024). Polycatenated Architected Materials.
2. Junjun, Feng & Wang, Enyuan & Shen, Rongxi & Chen, Liang & Li, Xuelong & Xu, Zhaoyong. (2016). Investigation on energy dissipation and its mechanism of coal under dynamic loads. Geomechanics and Engineering. 11. 657-670. 10.12989/gae.2016.11.5.657.

3. Das, Soukat Kumar & Das, Arghya. (2020). Strain-rate dependent energy redistribution during isotropic confined comminution. Géotechnique Letters. 10. 1-24. 10.1680/jgele.20.00039.

Acknowledgments
I thank Prof. Chiara Daraio, Wenjie Zhou, and Sujeeka Nadarajah for their mentorship. I thank Robert T. Herzog for his financial support. I acknowledge that Jabri Garcia-Jimenez and I worked together on this project. Jabri is writing a paper on the latter half of the project.